Biomedicine & Pharmacotherapy 109 (2019) 322–332

Contents lists available at ScienceDirect

Biomedicine & Pharmacotherapy

journal homepage: www.elsevier.com/locate/biopha

A proteomic analysis of the anti-dengue virus activity of andrographolide

Atchara Paemanee[a,b], Atitaya Hitakarun[a], Phitchayapak Wintachai[a], Sittiruk Roytrakul[b], Duncan R. Smith[a,*]

[a] Molecular Pathology Laboratory, Institute of Molecular Biosciences, Mahidol University, 25/25 Phuttamonthon Sai 4, Salaya, Nakorn Pathom 73170, Thailand
[b] Proteomics Research Laboratory, Genome Technology Research Unit, National Center for Genetic Engineering and Biotechnology, National Science and Technology Development Agency, 113 Thailand Science Park, Phahonyothin Road, Khlong Nueng, Khlong Luang, Pathumthani 12120, Thailand

ARTICLE INFO

Keywords:
Andrographolide
Dengue virus
Glucose regulated protein 78
Proteomics

ABSTRACT

Andrographolide is a major bioactive constituent of *Andrographis paniculata* that has been shown in vitro to have antiviral activity against a number of viruses, including the mosquito transmitted dengue virus (DENV). However, how andrographolide exerts an anti-DENV effect remains unclear. This study therefore sought to further understand the mechanism of action of andrographolide in inhibiting DENV infection of liver cells using a proteomic based approach. Both 1 dimension (D) and 2D proteome systems were used. Initial data was generated through andrographolide treatment of HepG2 cells without DENV infection (1D analysis), while subsequent data was generated through a combination of andrographolide treatment and DENV infection (2D analysis). A total of 17 (1D) and 18 (2D) proteins were identified as differentially regulated. The analyses identified proteins involved in chaperone activities, as well as energy production. In particular evidence suggested an important role for GRP78 and the unfolded protein response in mediating the anti-DENV activity of andrographolide, which might, in part, explain the broad antiviral activity of andrographolide.

1. Introduction

Dengue virus (DENV) is an enveloped, positive sense single-stranded RNA virus in the family *Flaviviridae*, genus *Flavivirus*, species *Dengue virus* [1]. It is transmitted to humans by *Aedes* species mosquitoes during a blood meal, and human infection can result in a range of symptoms from an acute self-limiting febrile illness, to life-threatening dengue hemorrhagic fever (DHF) and dengue shock syndrome (DSS) [2]. While the tissue tropism of DENV infection remains poorly defined, the involvement of the liver in the disease has been well established (reviewed in [3]) and both mouse model systems [4] and human autopsy studies [5] support the involvement of the liver in DENV infection, with hepatocytes being identified as the primary cell type infected and a site of DENV replication. The involvement of the liver is reflected by increased levels of the liver enzymes ALT and AST in DENV infection [6], suggestive of liver damage as a consequence of DENV infection. Thus anti-dengue therapeutics targeted towards the liver may serve to both diminish the total disease burden, as well as provide additional hepatoprotection.

Andrographis (A.) paniculata (Burm. f.) Wall. ex Nees is a medicinal plant commonly used in traditional medicine over much of Asia for treatment of a number of conditions including fever, a common symptom of DENV infection [7,8]. The bitter taste of all parts of the plant is reflected in the common name of *A. paniculata*, namely the "King of Bitters". Extracts of *A. paniculata* have a variety of pharmacological properties, including anticancer, anti-inflammatory, immunomoduratory, anti-viral, hypoglycaemic, cardioprotective, and hepatoprotective [7]. Phytochemical studies have shown that *A. paniculata* has a large number of flavonoids, stigmasterols, xanthones and labdane diterpenoids. Of the latter compounds, andrographolide (3α, 14, 15, 18-tetrahydroxy-5β, 9βH, 10α-labda-8, 12-dien-16-oic acid γ-lactone) was shown to be a major bioactive phytoconstituent of *A. paniculata* [7].

Significant anti-viral activity of andrographolide has been shown for a number of viruses including influenza A [9], dengue virus [10,11], chikungunya virus [12], hepatitis B virus [13], hepatitis C virus [14], herpes simplex virus [15,16] and human immunodeficiency virus [17,18]. However, the mechanism by which andrographolide exerts its anti-viral effect remains unclear. Andrographolide has been shown to directly bind to host cell proteins such as actin and NF-κB [19] and may thus exert its effect through these proteins as proposed elsewhere [10]. However, andrographolide has been shown to modulate a number of

* Corresponding author at: Institute of Molecular Biosciences, Mahidol University, Salaya Campus, 25/25 Phuttamonton Sai 4, Salaya, 73170 Nakorn Pathom, Thailand.
E-mail address: duncan.smi@mahidol.ac.th (D.R. Smith).

https://doi.org/10.1016/j.biopha.2018.10.054
Received 7 July 2018; Received in revised form 10 October 2018; Accepted 10 October 2018

cellular processes including autophagy [13,20], mitochondrial function [21], the unfolded protein response (UPR) pathway [22,23], and oxidative stress [24]. Thus andrographolide may have broad effects within the cell, with multiple pathways affected resulting in multiple antiviral effects. To explore further the antiviral activity of andrographolide, the anti-DENV activity of andrographolide was investigated using proteomic approaches.

2. Materials and methods

2.1. Cells lines and viruses

The human liver cell line HepG2 (ATCC Cat No. HB-8065) was cultured in Dulbecco's modified Eagle's medium (DMEM; Gibco BRL, Gaitherburg, MD) supplemented with 10% (v/v) heat inactivated fetal bovine serum (FBS; Gibco BRL, Gaitherburg, MD) at 37 °C with 5% CO_2. Dengue virus serotype 2 (DENV 2; strain 16,681) was propagated in the *Aedes albopictus* derived cell line C6/36 (ATCC No. CRL-1660) as described previously [25]. Virus supernatant was centrifuged at 1000xg to remove cell debris, supplemented to a final concentration of 20% (v/v) FBS and stored frozen at -80° C. Virus titer was determined by standard plaque assay on LLC-MK_2 cells (ATCC No. CCL-7) essentially as described previously [25].

2.2. Andrographolide

Andrographolide (365,645; Sigma-Aldrich, St. Louis, MO) was dissolved in 100% DMSO to a final stock concentration of 100 mM and stored at -30° C. Compound was diluted to various concentrations using complete DMEM supplemented with 10% FBS. The final concentration of DMSO in media was less than 0.2%.

2.3. Andrographolide treatment of cells

HepG2 cells were seeded into six well culture plates and grown until the cells reached approximately 90% confluency. The cells were washed with PBS and infected or mock infected with DENV 2 at a multiplicity of infection (MOI) of 5 at 37° C for 2 h in the absence of FBS. The cells were washed with PBS and then incubated with andrographolide at various concentrations (50, 100, and 200 μM) or incubated with a relevant DMSO control (no treatment control). Cells were incubated under standard conditions until analyzed. Cytotoxicity of andrographolide was determined using Alarmar Blue as previously described [12].

2.4. Flow cytometry

Mock- or DENV 2 infected cells (with or without andrographolide treatment as appropriate) were harvested at appropriate times and then incubated with 10% normal goat serum (Gibco BRL, Gaithersburg, MD) in PBS on ice for 30 min. The cells were washed with 1 ml of PBS followed by fixing with 200 μl of 4% paraformaldehyde in PBS at room temperature in the dark for 20 min. After washing twice with 1 ml of 1% BSA in PBS-IFA (0.5 M Na_2HPO_4, 0.5 M KH_2PO_4, 1.5 M $NaCl_2$), the cells were permeabilized with 200 μl of 0.2% Triton X-100 in PBS-IFA for 10 min. Subsequently, the cells were washed twice with 1 ml of 1% BSA in PBS-IFA followed by overnight incubation with 50 μl of a pan specific mouse anti-dengue virus monoclonal antibody from hybridoma HB114 [26] diluted 1:150 in 1% BSA/PBS-IFA at 4° C. After washing twice with 1 ml of 1% BSA in PBS-IFA, the cells were incubated with 50 μl of a goat anti-mouse IgG antibody conjugated with fluorescein isothiocyanate (FITC; 02-18-06; KPL, Guilford, UK) diluted 1:40 in 1% BSA in PBS-IFA for 1 h at room temperature in the dark. The cells were then washed twice with 1 ml of 1% BSA in PBS-IFA and resuspended in 200 μl of PBS-IFA. The fluorescence signal was analyzed by flow cytometry on a BD FACalibur cytometer (Becton Dickinson, BD Biosciences, San Jose, CA) using CELLQuest™ software. All experiments were undertaken independently in triplicate.

2.5. One-dimensional (1D)-gel electrophoresis and liquid chromatography–tandem mass spectrometry (GelC–MS/MS)

Determination of protein concentration was performed by the Bradford assay [27]. Protein samples were electrophoresed though 12% SDS PAGE gels. Subsequently each sample lane was separated into 10 slices. Each slice of the gel was diced into cubes of approximately 1 mm^3. All gel pieces were subjected to in-gel tryptic digestion using an in-house method modified from Shevchenko and colleagues [28], essentially as described elsewhere [29]. Briefly, the gel plugs were dehydrated with 100% acetonitrile (ACN), reduced with 10 mM DTT in 10 mM ammonium bicarbonate at 56° C for 1 h and alkylated at room temperature for 1 h in the dark in the presence of 100 mM iodoacetamide in 10 mM ammonium bicarbonate. After alkylation, the gel pieces were dehydrated with 100% ACN for 5 min. To perform in-gel digestion of protein sample, 100 ng of trypsin (10 ng/μl trypsin in 10 mM ammonium bicarbonate) was added followed by incubation at room temperature for 5 min, and then 20 μl of 10 mM ammonium bicarbonate was added to keep the gel pieces immersed throughout the digestion. The gel pieces were incubated at 37° C for 3 h. To extract digested peptides, 30 μl of 50% ACN in 0.1% formic acid was added into the gels, and then the gel pieces were incubated at room temperature for 10 min with vigorous shaking. The extracted peptides were collected and pooled together in a new tube. The pooled-extracted peptides were dried at 40° C and kept at -80° C for further analysis. Finally, dried samples were dissolved in 0.1% formic acid for subsequent mass spectrometry analysis. MS/MS analysis of tryptic peptides was performed using a SYNAPT HDMS mass spectrometer (Waters Corp., Manchester, UK). For all measurements, the mass spectrometer was operated in the V-mode of analysis with a resolution of at least 10,000 full-width half-maximum. All analyses were performed using the positive nanoelectrospray ion mode. The time-of-flight analyzer of the mass spectrometer was externally calibrated with [Glu^1]fibrinopeptide B from *m/z* 50 to 1600 with acquisition lock mass corrected using the monoisotopic mass of the doubly charged precursor of [Glu^1]fibrinopeptide B. The reference sprayer was switched at a frequency of 20 s. Accurate mass LC–MS data were acquired with the data direct acquisition mode. The energy of the trap was set at a collision energy of 6 V. In transfer collision energy control, low energy was set at 4 V. The quadrupole mass analyzer was adjusted such that ions from *m/z* 300 to 1800 were efficiently transmitted. The MS/MS survey was over the range 50 to 1990 Da and scan time was 0.5 s. For proteins quantitation, DeCyder MS Differential Analysis software (DeCyderMS, GE Healthcare) was used.

2.6. Two-dimensional (2D)-gel electrophoresis and liquid chromatography-mass spectrometry

Two-dimensional gel electrophoresis experiments were all performed as three independent biological replicates. A total of 165 μg of total proteins were premixed with a rehydration solution containing 7 M Urea, 2% CHAPS, 2% ampholytes (pH 3–10), 120 mM DTT, 40 mM Tris-base and bromophenol blue and loaded onto an immobilized pH gradient (IPG) strip (7 cm, nonlinear pH 3–10; GE Healthcare). The IPG strips were incubated in an equilibration buffer containing 30% glycerol, 20% sucrose, 2% SDS, 50 mM Tris − HCl (pH 8.8), 100 mM DTT, and 0.002% bromophenol blue overnight. Isoelectric focusing was performed using an IPGphor IEF system (GE Healthcare, Buckinghamshire, UK) at 50 mA per strip at 20 °C using a continuous increase in voltage (up to 5000 V) to reach 12,100 V h. The second dimension electrophoresis was conducted on a vertical electrophoresis system. The equilibrated IPG strips were placed onto the top of a 12.5% SDS-PAGE gel and the samples were resolved with a constant voltage of

100 V for 2.5 h.

Comparative analysis of protein spots was performed using Image Master 2D Platinum software version 7.0 (GeneBio, Switzerland). Candidate spots were only included if they were consistently detected in all three replicate gels. Background subtraction was performed, and the intensity volume of each spot was normalized with total intensity volume (summation of the intensity volumes obtained from all spots within the same 2D gel). After spot analysis, the protein spots with significant changes in intensity volume (One way ANOVA; $p < 0.05$) and with a ratio of normalized volume intensity, of more than 1.5-fold different were excised with a sterile scalpel for subsequent in-gel digestion and mass spectroscopic analysis.

2.7. MS data analysis

Acquired LC–MS raw data were converted and the PepDetect module was used for automated peptide detection, charge state assignments, and quantitation based on the peptide ions signal intensities in MS mode. The MS/MS data from DeCyderMS were submitted to a database search using the Mascot software (Matrix Science, London, UK). The data was searched against the NCBI database for protein identification. Database was; taxonomy (Homo sapiens); enzyme (trypsin); fix modification (carbamidomethylation of cysteine); variable modifications (oxidation of methionine residues, deamidated NQ, acetyl N-term); mass values (monoisotopic); protein mass (unrestricted); peptide mass tolerance (1.2 Da); fragment mass tolerance (± 0.6 Da), peptide charge state (1+, 2+ and 3+) and max missed cleavages.

Functional analysis of identified proteins was undertaken using PANTHER version 12.0 [30], the DAVID Bioinformatics Resource 6.8 [31,32], and STRING 10.5 (Search Tool for the Retrieval of Interacting Genes/Proteins) 10.5 [33].

2.8. Western blot analysis

HepG2 cells after appropriate treatment or control treatment were packed by centrifugation at 1600 rpm for 5 min then washed with 1 ml of 1x PBS. Cells were centrifuged again at 1600 rpm for 5 min and cell pellets were lysed in 250 µl of RIPA buffer. The cell suspensions were chilled on ice for 5 min and mixed again by vortexing. Physical disruption of cell suspensions was performed by sonication for 7 min followed by incubation on ice. The suspensions were mixed and sonicated twice more until clear lysate solution was obtained. Suspensions were centrifuged at 13,000 rpm for 15 min at 4 °C before the protein concentration was determined by the Bradford assay [27]. Proteins were separated by electrophoresis though 12% SDS-polyacrylamide gels and transferred to solid matrix support. Filters were probed with antibodies directed against heat shock protein 90 (HSP90), heat shock protein 70 (HSP70), glucose regulated protein 78 (GRP78), eukaryotic initiation factor 2 alpha subunit (eIF2α), phospho-eIF2α, prohibitin, voltage-dependent anion-selective channel (VDAC), protein disulfide isomerase family A member 6 (PDIA6), Solute carrier family 2, facilitated glucose transporter member 1 (SLC2A1), heat shock cognate 71 kDa protein 8 (HSPA8), NF-κB (p50 subunit), phospho-(pS773)-NF-κB (p50 subunit), glyceraldehyde 3-phosphate dehydrogenase (GAPDH), heat shock protein 60 (HSP60), PERK, phospho-PERK, LC3 and viral proteins (DENV E, NS1 and NS5) using specific antibodies followed by a suitable dilution of a suitable HRP conjugated secondary antibody (see Supplementary Table 1). Signals were developed using the Clarity western ECL substrate (Bio-Rad, Hercules, CA). All experiments were undertaken as three independent biological replicates, and the band intensity of the signals was determined using Quantity One 1D analysis software (Bio-Rad, Hercules, CA).

2.9. Total RNA extraction and qRT-PCR

Total RNA was isolated with TRIzol reagent (Life Technologies Inc., Carlsbad, CA) according to the manufacturer's procedure. RNA concentration was measured by a Nanodrop-2000 (Thermo Fisher Scientific Inc., Wilmington, DE), and sample purity was verified by using the absorbance ratio at OD 260/280 which for all samples was in the range of 1.8-2.0. Genomic DNA was removed by DNase I (Life Technologies Inc.) treatment and re-extraction of the treated RNA with TRIzol reagent. The extracted RNA was used as a template for cDNA synthesis using RevertAid Reverse Transcriptase (Thermo Fisher Scientific Inc., Waltham, MA). The reverse transcription PCR was undertaken using a VeritiTM Thermo Cycler (Applied Biosystems, Foster City, CA) and the reaction contained 1 µg total RNA, 1 µM random hexamers, 1X reaction buffer and 200 U RevertAid Reverse Transcriptase. Gene expression levels were determined by qPCR and the reaction contained 5 ng cDNA, 1X KAPA SYBR FastMaster Mix (Kapa Biosystems, Inc., Wilmington, MA) and 300 nM of each specific primer as described in Supplementary Table 2. These reactions were carried out using a Mastercycler realplex (Eppendorf AG, Hauppauge, NY) with an initial denaturation at 95 °C for 3 min and then denaturation at 95 °C for 10 s, annealing at 60 °C for 30 s and extension at 72 °C for 20 s for 40 cycles. Expression of GAPDH, GRP78, HSP60 and actin were assessed at 12, 24, 36 h. The expression of RNA was normalized against actin and the RNA expression level was calculated by using the 2-ΔΔCT method (ΔΔCT = ΔCTtreat - ΔCTcontrol, ΔCT = Ct gene - Ct actin).

2.10. Statistical analysis

All data were analyzed using the GraphPad Prism program (GrapPad Software Inc., San Diego, CA). Statistical analysis of significance was undertaken by One-Way ANOVA on raw data reads using SPSS (SPSS Inc., Chicago, IL). Real time PCR data was evaluated by independent sample *t*-tests. Data was considered as statistically significant at a *p*-value of less than 0.05.

3. Results

3.1. GeLC-MS/MS analysis of HepG2 cells treated with andrographolide

To attempt to understand how andrographolide exerts its anti-viral effect, gel-enhanced liquid chromatography coupled with tandem mass spectrometry (GeLC-MS/MS) was utilized. HepG2 cells were therefore treated with 100 µM andrographolide or with vehicle (DMSO) in three independent replicates and at 24 h post treatment cells were harvested, and total proteins prepared, pooled and subjected to separation by SDS-PAGE electrophoresis. Sample lanes were divided into ten slices and proteins were subjected to in-gel tryptic digestion followed by tandem mass spectrometry. More than 1500 peptides were detected and analyzed, of which six hundred and fifty eight peptides were differentially present with a *p*-value of ≤ 0.05. There was no the obvious difference of expression between andrographolide treated HepG2 cells and control. The ratio of expression range from 0.84 to 1.37 and the changes existed between ± 0.03 and ± 0.37. Final protein identification was based on the presence of at least 2 peptides per protein, and using this criterion a total of 17 differentially expressed proteins were identified from the *Homo sapiens* database (Table 1).

3.2. Ontological analysis of proteins differentially expressed after andrographolide treatment of HepG2 cells

Ontological analysis using the DAVID Bioinformatics resource [31,32] generated 5 annotation clusters with enrichment scores ranging from 3.52 to 1.04. Cluster 1 contained terms related to protein post-translational modification (e.g. ubiquitin-like modifier proteins, methylation, isopeptide bond), while cluster 2 contained terms related to

Table 1
Differentially expressed proteins identified after andrographolide treatment of HepG2 cells.

No.	Protein name	Uniprot Accession	Score	No. of peptides/ expression	Representative Intensity		
					100 μM ANDRO	0.1% DMSO	Fold change (ANDRO/ 0.1%DMSO)
1	histone H4	P62805	50.54	3/down	9.88	11.76	0.84
2	40S ribosomal protein S25	P62851	34.16	2/ND	–	–	–
3	enhancer of rudimentary homolog	P84090	34.51	2/down	5.60	6.27	0.89
4	nucleoside diphosphate kinase A isoform a	P15531	53.49	3/ND	–	–	–
5	heat shock cognate 71 kDa protein	P11142	59.3	3/up	9.92	7.22	1.37
6	dehydrogenase/reductase SDR family member 2, mitochondrial isoform 2	Q13268	31.54	4/up	8.44	7.60	1.11
7	heat shock 70 kDa protein 1 A	P0DMV8	55.39	6/up	9.79	0.00	ND
8	L-lactate dehydrogenase A chain isoform 4	P00338	39.95	3/ND	–	–	–
9	glyceraldehyde-3-phosphate dehydrogenase isoform 1	P04406	49.86	3/down	10.45	10.67	0.97
10	protein disulfide-isomerase A6 isoform b	Q15084	77.28	2/up	8.23	6.13	1.34
11	keratin, type II cytoskeletal 8 isoform 2	P05787	62.76	3/up	10.02	8.53	1.17
12	glucose transporter glycoprotein	P11166	57.45	2/up	8.81	6.59	1.34
13	beta-tubulin	P07437	33.16	3/down	9.23	9.93	0.93
14	UDP-glucose 6-dehydrogenase isoform 2	O60701	70.98	2/down	10.32	11.10	0.93
15	heat shock protein 90 kDa beta (Grp94)	P14625	60.46	4/up	10.16	9.69	1.05
16	78 kDa glucose-regulated protein precursor	P11021	36.21	3/down	9.25	10.32	0.88
17	heat shock protein 60	P10809	76.41	7/up	12.88	11.80	1.09

Table 2
List of 18 proteins identified as differentially expressed in 2D analysis of HepG2 cells infected and/or treated with andrographolide or vehicle.

Spot No.	Protein name	Uniprot Accession	score	%COV	Intensity						p
					Mock Infection			Infection			
					DMSO	ANDRO	Ratio	DMSO	ANDRO	Ratio	
7	Dehydrogenase/reductase SDR family member 2, mitochondrial	Q13268	42	16	3756.33	8946.00	2.38	11258.3	9231.67	0.82	0.0035
50	Chloride intracellular channel protein 1	O00299	201	33	11541.30	13980.00	1.21	5968.33	8944.00	1.50	0.00034
85	Voltage-dependent anion-selective channel protein 2	P45880	62	8	6104.33	4455.67	0.73	5918.00	6233.00	1.05	0.017
91	Glyceraldehyde-3-phosphate dehydrogenase	P04406	115	20	14629.00	28869.30	1.97	10368.70		0.00	0.00019
92	Aldo-keto reductase family 1 member C1	Q04828	89	12	15348.30	30062.70	1.96	9063.33	22704.00	2.51	9.78E-07
107	Fructose-bisphosphate aldolase A	P04075	303	32	12019.00	18446.00	1.53	20210.70	27672.30	1.37	0.0073
112	26S proteasome non-ATPase regulatory subunit 13	Q9UNM6	34	5	7344.33	6214.67	0.85	2365.00	1267.00	0.54	0.0063
133	Isocitrate dehydrogenase [NADP] cytoplasmic	O75874	113	15	5896.33	2547.67	0.43	2828.33	0.00	0.00	0.00025
136	Alpha-enolase	P06733	49	8	5061.33	4392.33	0.87	5356.00	0.00	0.00	0.0020
145	Citrate synthase, mitochondrial	O75390	29	4	17830.70	12487.70	0.70	13179.00	10747.00	0.82	0.050
170	Glutamate dehydrogenase 1, mitochondrial	P00367	115	9	23681.00	18115.00	0.76	24087.00	17859.70	0.74	0.0063
179	D-3-phosphoglycerate dehydrogenase	O43175	7.3	6	14011.00	11264.30	0.80	13186.70	9617.00	0.73	0.038
221	ATP synthase subunit beta, mitochondrial	P25705	284	22	8557.67	7606.00	0.89	5581.67	1598.67	0.29	0.029
224	60 kDa heat shock protein, mitochondrial	P10809	79	3	11581.30	9380.67	0.81	6670.67	5473.00	0.82	0.037
329	Serotransferrin	P02787	114	10	11214.30	6335.67	0.56	10529.00	6853.00	0.65	0.031
357	Succinate dehydrogenase [ubiquinone] flavoprotein subunit, mitochondrial	P31040	52	1	6095.33	4065.67	0.67	5526.00	3083.00	0.56	0.028
418	78 kDa glucose-regulated protein	P11021	691	30	43903.00	42407.00	0.97	43772.00	40403.00	0.92	0.0098
458	Far upstream element-binding protein 1	Q96AE4	141	11	2703.00	5171.00	1.91	4633.00	3987.67	0.86	0.039

chaperone like activities (unfolded protein binding, chaperone, stress response). The other clusters were related to the endoplasmic reticulum (cluster 3), oxidation-reduction processes (cluster 4) and assorted processes (identical protein binding, biosynthesis of antibiotics and metabolic pathways; cluster 5). The full list of terms and enrichment factors is given in Supplemental File 1. It is interesting that 5 of the proteins (heat-shock cognate 71 kDa protein, heat shock 70 kDa protein 1 A variant, heat shock protein 90 kDa beta (GRP94), 78 kDa glucose-regulated protein precursor (GRP78) and heat shock protein 60) are chaperone or chaperonin proteins associated with protein folding. STRING analysis [33] identified 16 biological process pathways (Supplemental File 2) including response to unfolded protein (5 proteins; false discovery rate 0.00109), response to stress (10 proteins; false discovery rate 0.032) and response to chemical (10 proteins; false discovery rate 0.0475), Fig. 1. The overall protein-protein interaction (PPI) enrichment p-value was 3.27×10^{-10}, indicating a degree of functional biological connectedness of the identified proteins.

3.3. Validation of GelC-MS/MS protein expression results

Based on the results of the GelC-MS/MS, four proteins (HSPA8, PDIA6, SLC2A1 and GRP78) were selected for validation, together with investigation of another six proteins (Prohibitin, VDAC, HSP70, HSP90, eIF2α, NF-κB) that were selected based upon candidate protein criteria. To validate the involvement of these proteins as part of the response to andrographolide treatment, HepG2 cells were either not treated or treated with 100 or 200 μM andrographolide for 24 h, after which proteins were prepared and separated by SDS-PAGE. After transfer to solid matrix support the expression levels of prohibitin, HSP70, PDIA6, HSPA8, HSP90, SLC2A1, VDAC and GRP78, together with the degree of phosphorylation of eIF2α and NF-κB p50 (pS337) were determined by western blotting. Membranes were additionally probed with an antibody against actin as an internal control. Experiment was undertaken as three independent biological replicates.

Results (Fig. 2) showed a significant increase in the expression of

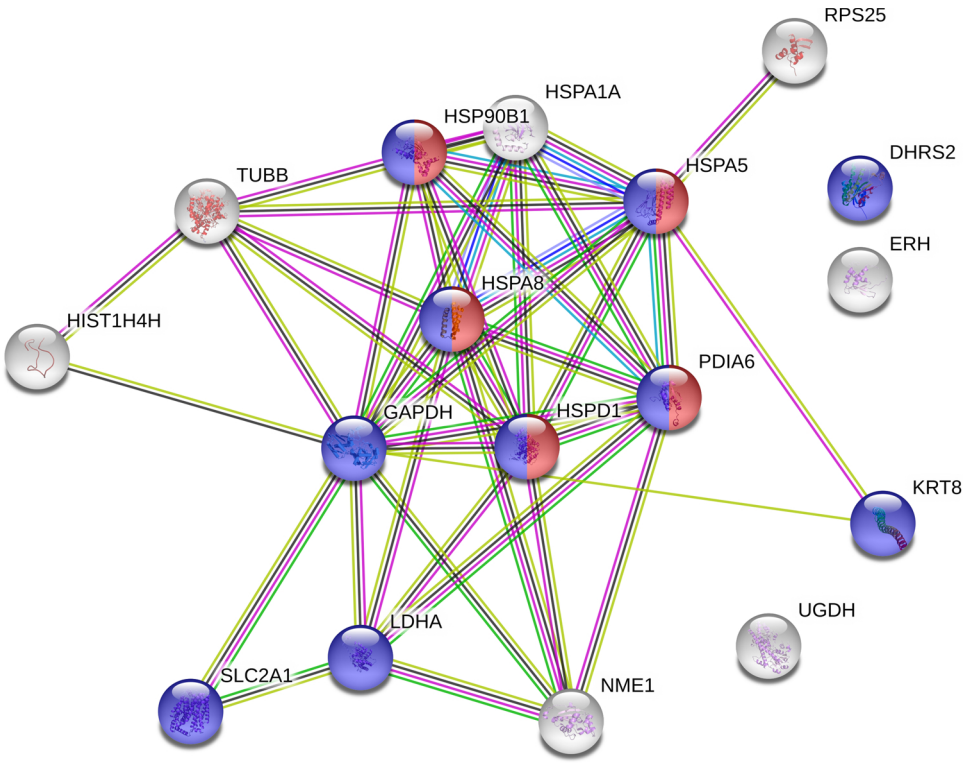

Fig. 1. STRING analysis of 17 proteins altered in response to andrographolide. (For interpretation of the references to color in this figure legend, the reader is referred to the web version of this article.)
A total of 17 proteins identified as differentially expressed in response to andrographolide were submitted to the STRING database for analysis. Proteins identified as part of the response to unfolded protein are shown in red, while proteins identified as part of the response to stress are shown in blue. Proteins involved in both processes are shown as dual coloured.

HSP70 and PDIA6 in response to andrographolide treatment (consistent with the results of the GeLC-MS/MS), as well as a significant reduction in expression of HSP90, SLC2A1 and VDAC. Phosphorylation of eIF2α was significantly increased by treatment with 200 μM andrographolide, and while NF-κB showed a dose dependent reduction in phosphorylation in response to andrographolide, it did not reach statistical significance.

Increased phosphorylation of eIF2α is mediated by the ER resident protein kinase RNA-like endoplasmic reticulum kinase (PERK). Under conditions of ER stress, the unfolded protein response (UPR) is activated leading to oligomerization and autophosphorylation of PERK amongst other events [34]. We therefore assessed the phosphorylation status of PERK and observed a significant increase in PERK phosphorylation in response to andrographolide treatment (Fig. 3).

3.4. Effects of andrographolide on DENV 2 infection

We have previously shown that andrographolide treatment can significantly reduce DENV infection, and moreover we have established that andrographolide only has activity at a post-infection stage [10], which was also seen with the antiviral activity against chikungunya virus [12]. To further understand the mechanism of action of

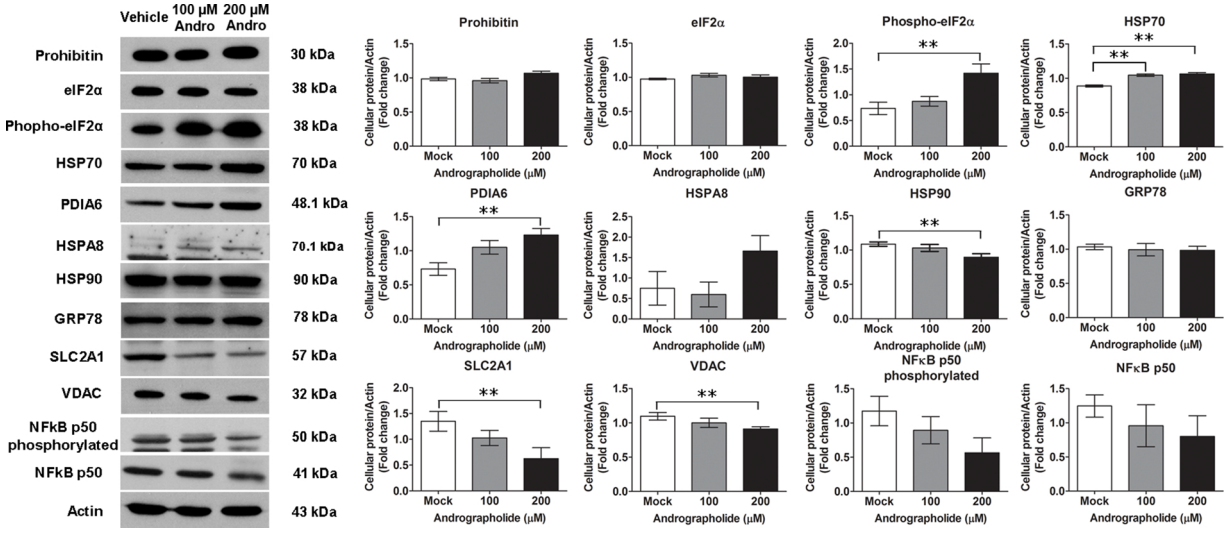

Fig. 2. Effect of andrographolide treatment on HepG2 cells.
(A) HepG2 cells were treated with 100 or 200 μM of andrographolide (ANDRO) or with vehicle for 24 h and proteins prepared and subjected to western blot analysis to detect the expression of prohibitin, eIF2α, phospho-eIF2α, HSP70, PDIA6, HSPA8, HSP90, SLC2A1, VDAC, GRP78, NF-κB p50 and phospho-NF-κB p50. Experiment was undertaken independently in triplicate and representative blots are shown. (B) Protein band intensities from (A) were quantitated using Quantity One and the expression all proteins was normalized to actin. Error bars represent S.E.M. (**; p value < 0.05).

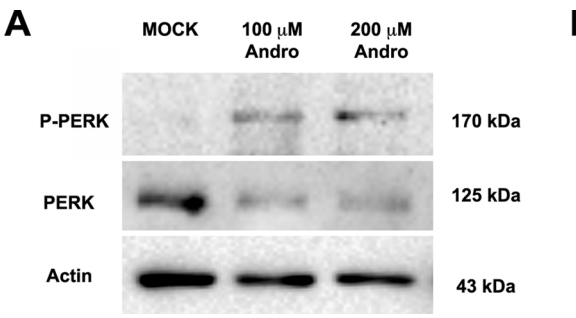

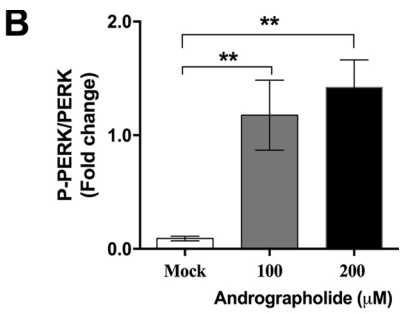

Fig. 3. Effect of andrographolide treatment on PERK phosphorylation.
(A) HepG2 cells were treated with 100 or 200 μM of andrographolide (ANDRO) or with vehicle for 24 h (mock) and proteins prepared and subjected to western blot analysis to detect the expression phospho-PERK (p-PERK), PERK and actin. Experiment was undertaken independently in triplicate and representative blots are shown. (B) Protein band intensities for (A) were quantitated using Quantity One and p-PERK expression was normalized to PERK. Error bars represent S.E.M. (**; p value < 0.05).

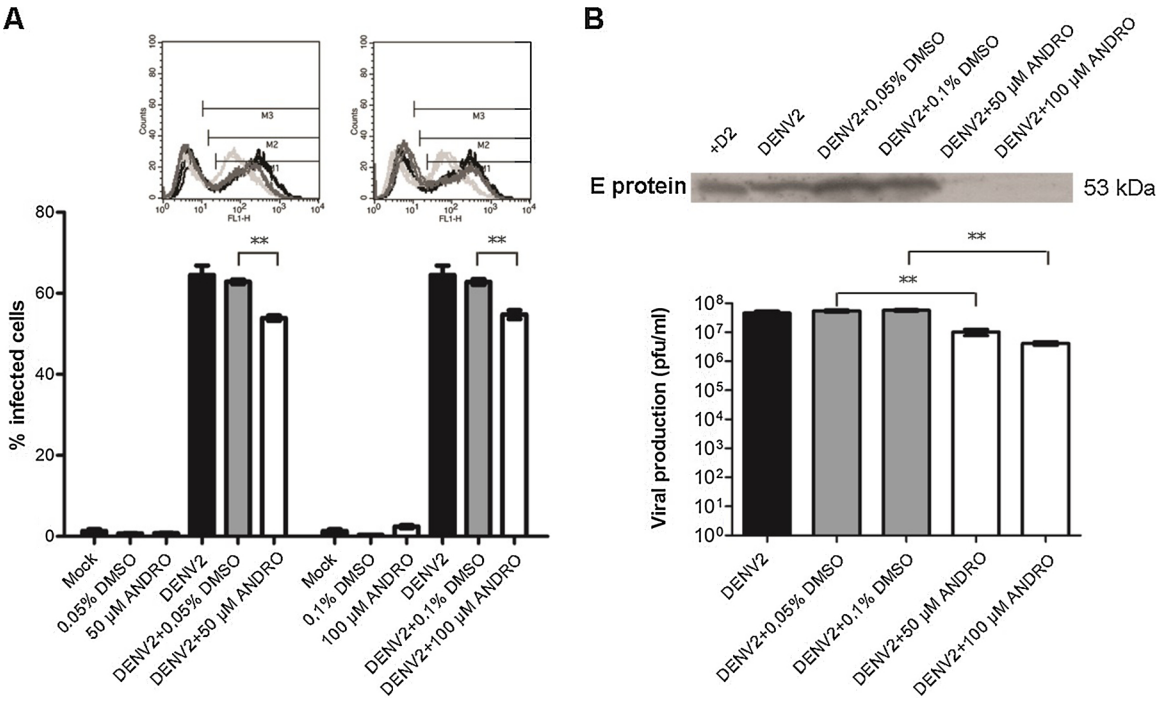

Fig. 4. Effect of andrographolide on DENV 2 infection of HepG2 cells.
HepG2 cells were infected or mock infected with DENV 2 followed by incubation with 50 or 100 μM andrographolide (ANDRO) or with vehicle under standard conditions for 24 h. The level of infection was determined by (A) flow cytometry. Experiment was undertaken independently in triplicate. Black bars DENV 2 infection only, grey bars, DENV 2 infection and treatment with vehicle, white bars DENV 2 infection and treatment with andrographolide. (B) Viral protein expression in the supernatant was determined by western blotting, and viral production was determined by standard plaque assay. Experiments were performed independently in triplicate, with duplicate plaque assay. Error bars represent S.E.M. (**; p value < 0.05)

andrographolide, a further proteomic analysis was undertaken. We initially confirmed the ability of andrographolide to reduce both the percentage of cells infected, as well as the virus output and to reduce structural protein production. HepG2 cells were therefore mock infected or infected with DENV 2 and subsequently treated with either vehicle alone or andrographolide at concentrations of 50 and 100 μM. At 24 h.p.i cells were analyzed by flow cytometry while the supernatant was analyzed by standard plaque assay and western blotting to detect DENV 2 E protein. Results (Fig. 4) showed significant reductions in the percentage of cells infected at both concentrations of andrographolide. Similarly, viral titer was significantly reduced and a clear reduction in E protein in the supernatant was observed by treatment at both concentrations (Fig. 4). Although as previously established andrographolide shows no cytotoxicity in HepG2 cells at concentrations up to 100 μM [10,12], the lower concentration (50 μM) was selected to undertake further proteomic analysis. To further justify this level of treatment with andrographolide, we determined the CC_{50} value of andrographolide in HepG2 cells to be 828.426μM, and additionally we note some cytotoxicity occurring at and above 200μM (Supplemental Fig. 1).

3.5. 2D-gel analysis of effects of andrographolide on DENV 2 infection

To determine the effects of andrographolide in DENV infection, four experimental conditions were established, namely HepG2 cells treated with vehicle alone, HepG2 cells treated with 50 μM andrographolide alone, HepG2 cells infected with DENV 2 and treated with vehicle and HepG2 cells infected with DENV 2 and treated with 50 μM andrographolide. Experiment was undertaken as three independent biological replicates. The cells were collected at 24 h.p.i, and proteins prepared. Prior to proteomic analysis, aliquots of the supernatant taken at 0 h (immediately post infection) and 24 h.p.i. were analyzed by standard plaque assay to confirm both that infection was successful and to verify the anti-DENV effect of andrographolide in this experiment. Results (Supplemental Fig. 2) showed a significant reduction in virus titer in response to andrographolide treatment as expected. Proteins from the four experimental conditions were therefore subjected to 2D-gel separation and gels were subsequently stained with Commassie

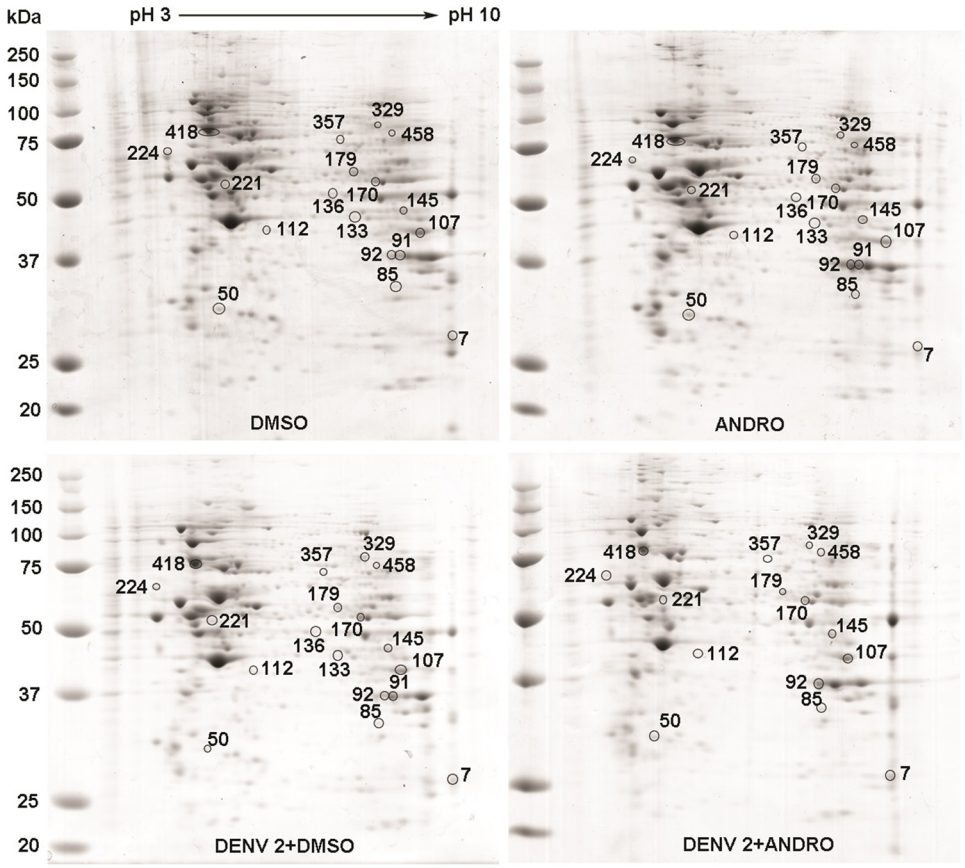

Fig. 5. 2D analysis of effects of andrographolide on DENV 2 infection of HepG2 cells.
HepG2 cells treated with vehicle alone (DMSO) or with 50 μM andrographolide alone (ANDRO) or DENV 2 infected and treated with vehicle (DENV2 + DMSO) or with 50 μM andrographolide (DENV2 + ANDRO) and after 24 h proteins were prepared and resolved by 2 dimensional gel electrophoresis and stained with Coomessie G250. Experiment was undertaken in three independent biological replicates, and representative gels are shown. Intensity of spots was analyzed using Image Master 2D Platinum software version 7.0. Differentially expressed spots were identified based on equality in the three replicate and with ANOVA ≤ p 0.05.

G250 (Fig. 5). The spots were analyzed and a total of 19 differentially expressed spots were identified. Differentially expressed spots were removed from the gel, and subjected to in-gel tryptic digestion and identification by mass spectrometry. A total of 18 proteins were identified (Table 2).

3.6. Ontological analysis of differentially expressed proteins from 2D-gel analysis

Ontological analysis using the DAVID bioinformatics resource [31,32] generated 9 functional annotation clusters, with enrichment scores ranging from of 6.11 to 1.49. Cluster 1 (enrichment score 6.11) contained terms relating to carbon metabolism, biosynthesis and metabolic pathways, while cluster 2 (enrichment score 4.53) contained terms related to oxidation-reduction processes. Other clusters contained terms related to the tricarboxylic acid cycle, glycolysis and mitochondria. The full list of terms and enrichment scores for all clusters can be found in Supplemental File 3.

STRING analysis [33] identified 19 biological process pathways (Supplemental File 4) including oxidation-reduction process (10 proteins; false discovery rate $1.36e^{-05}$), generation of precursor metabolites and energy (7 proteins; false discovery rate $9.93e^{-05}$) and tricarboxylic acid metabolic process (4 proteins; false discovery rate $9.93e^{-05}$), see Fig. 6. The overall protein-protein interaction (PPI) enrichment p-value was $6.37e^{-13}$, indicating a high degree of functional biological connectedness of the identified proteins. Overall, both DAVID and STRING largely identified proteins involved in energy metabolism (glycolysis, oxidation-reduction) and that are associated with mitochondria.

3.7. Validation of differentially expressed proteins from 2D- gel analysis

To confirm the 2D-gel analysis results, the same four experimental conditions were established, namely HepG2 cells treated with vehicle alone, HepG2 cells treated with 50 μM andrographolide alone, HepG2 cells infected with DENV 2 and treated with vehicle and HepG2 cells infected with DENV 2 and treated with 50 μM andrographolide. Experiment was undertaken as three independent biological replicates. At 24 h.p.i. cells were harvested and proteins extracted and transferred to solid matrix support before western blot analysis to determine expression of 7 proteins, namely DENV E, NS1 and NS5 proteins, as well as three proteins identified as differentially expressed in the proteomic analysis, namely GAPDH, GRP78, HSP60 in addition to actin as a control. Results (Fig. 7) showed that expression of the DENV structural and non-structural proteins was significantly reduced by andrographolide treatment in confirmation of our previous observations [10]. Expression of GAPDH and GRP78 was similarly down-regulated by andrographolide treatment of DENV infected cells. Markedly, treatment with andrographolide alone did not reduce the expression of these proteins. HSP60, which was identified as down-regulated by andrographolide treatment showed no significant change in expression.

3.8. Gene expression analysis

To determine further if the effects of andrographolide were occurring at the transcriptional level, the expression of GAPDH, GRP78 and HSP60 was examined by quantitative RT-PCR. The four conditions used in the proteomic analysis (HepG2 cells treated with vehicle alone, HepG2 cells treated with 50 μM andrographolide alone, HepG2 cells infected with DENV 2 and treated with vehicle and HepG2 cells infected with DENV 2 and treated with 50 μM andrographolide) were again repeated and RNA from infected cells analyzed at 12, 24 and 36 h post infection. Results (Fig. 8) showed that there was some regulation of expression of all three genes. Treatment of cells with andrographolide (as compared to vehicle treated cells) showed early up-regulation of HSP60 at 12 and 24 h, but no difference at 36 h. GAPDH was initially

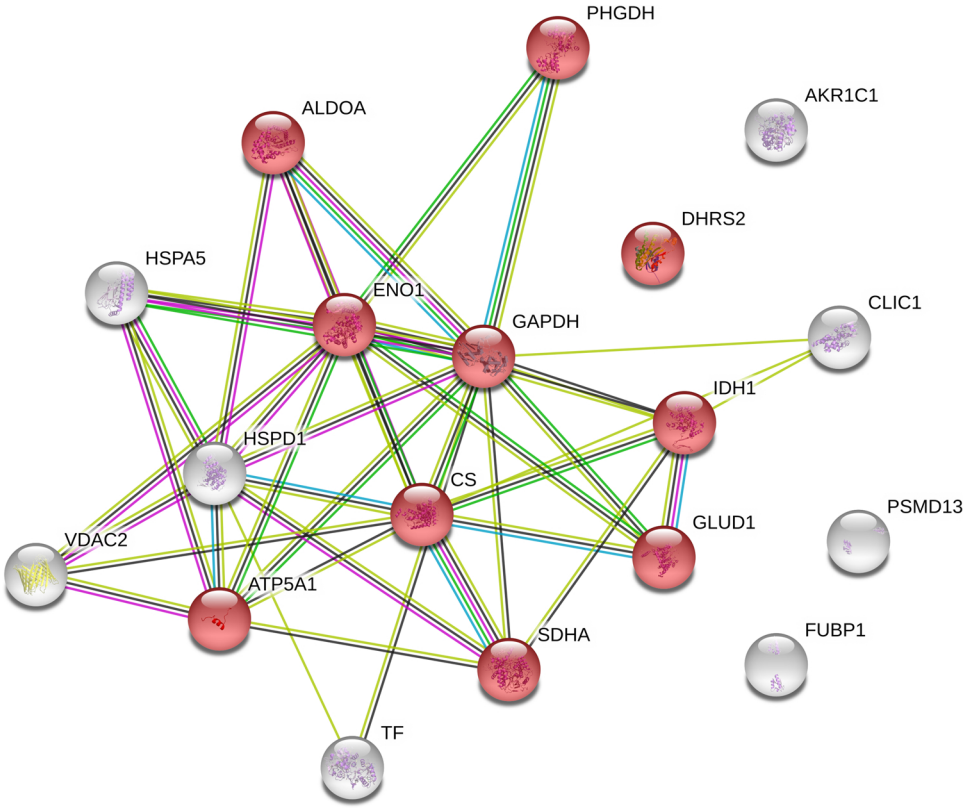

Fig. 6. STRING analysis of 18 proteins altered in response to DENV 2 infection and/or treatment with andrographolide or vehicle. (For interpretation of the references to color in this figure legend, the reader is referred to the web version of this article.)
A total of 18 proteins identified as differentially expressed in response to DENV 2 infection and/or treatment with andrographolide or vehicle were submitted to the STRING database for analysis. Proteins identified as part of the oxidation-reduction process are shown in red.

upregulated at 12 h post treatment, but was significantly down regulated at 24 h, and expression was unaffected at 36 h post treatment. GRP78 was not altered in expression at 12 h, but showed significant down-regulation at 24 and 36 h (Fig. 8). GRP78 was increased in dengue infected/andrographolide treated cells at 12 h, but significantly down-regulated at 24 and 36 h. GAPDH was only significantly altered at 24 h post treatment, when DENV infected/andrographolide treated cells showed increased expression as compared to dengue infected cells only.

3.9. Analysis of autophagy induction

It has been established that DENV infection results in the activation of autophagy [35,36], and similarly, andrographolide has been shown to induce autophagy [20,37,38]. To investigate the induction of autophagy, HepG2 cells were either mock infected, treated with vehicle (0.01% DMSO), treated with 100 μM andrographolide alone, infected with DENV 2, infected with DENV 2 in the presence of vehicle or infected with DENV 2 and treated with 100 μM andrographolide. At 24 h post treatment/infection cells were collected and proteins analyzed by western blot for the presence of the lipidated form of LC3 (LC3-II). Results (Fig. 9) showed the induction of autophagy in response to DENV infection consistent with previous studies [35,36], but treatment with andrographolide showed a very much larger increase in the presence of LC3-II as compared to cells infected with DENV alone.

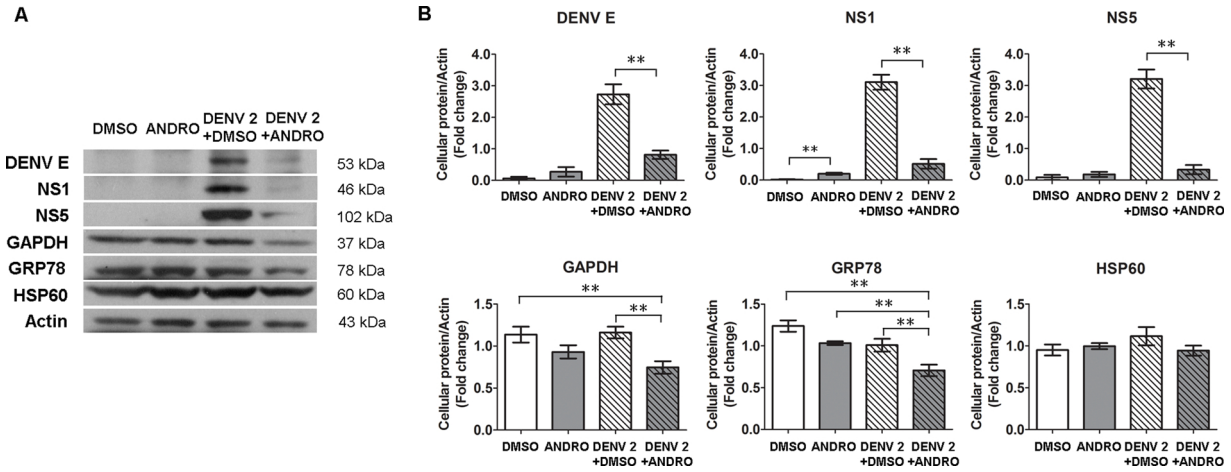

Fig. 7. Effect of andrographolide on protein expression in DENV 2 infected HepG2 cells.
HepG2 cells treated with vehicle alone (DMSO) or with 50 μM andrographolide alone (ANDRO) or DENV 2 infected and treated with vehicle (DENV2 + DMSO) or with 50 μM andrographolide (DENV2 + ANDRO) and after 24 h proteins were (A) prepared and subjected to western blot analysis to detect the expression of GAPDH, GRP78, HSP60 and viral proteins (DENV E, NS1 and NS5). The experiment was undertaken independently in triplicate and representative blots are shown. (B) Protein band intensities were quantitated using Quantity One and the expression all proteins was normalized to actin. Error bars represent S.E.M. (**; p value < 0.05)

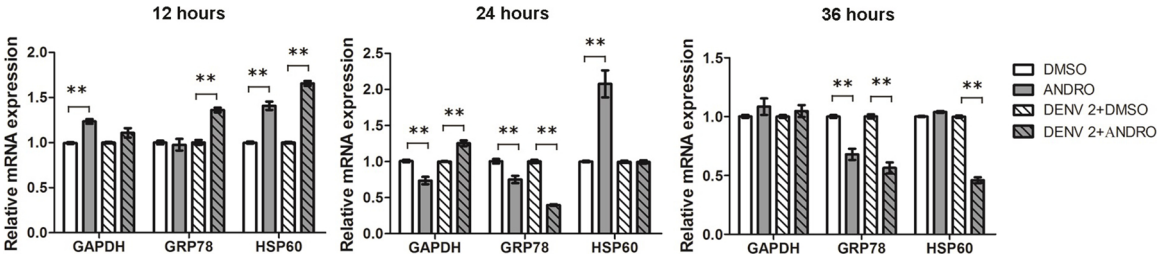

Fig. 8. Effect of andrographolide on gene expression in DENV 2 infected HepG2 cells.
HepG2 cells treated with vehicle alone (DMSO) or with 50 μM andrographolide alone (ANDRO) or DENV 2 infected and treated with vehicle (DENV2 + DMSO) or with 50 μM andrographolide (DENV2 + ANDRO) and after 12, 24 and 36 h total RNA was prepared and expression levels of GAPDH, GRP78, HSP60 and actin were determined by real time quantitative PCR. Expression of GAPDH, GRP78, HSP60 was normalized against actin. Error bars represent ± SD (**; p value < 0.05).

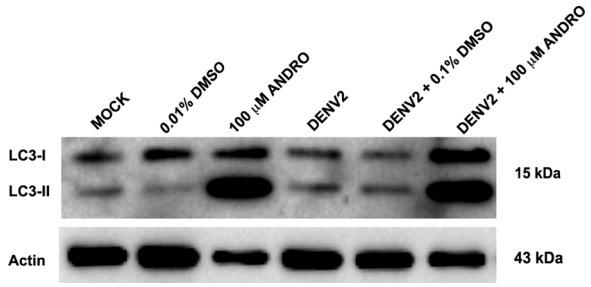

Fig. 9. Effect of andrographolide treatment on LC3 expression.
HepG2 cells were not treated (Mock) treated with vehicle alone (0.01% DMSO) or with 100 μM andrographolide alone (100 μM ANDRO) or DENV 2 infected alone (DENV2), or DENV2 infected and treated with vehicle (DENV2 + 0.1% DMSO) or with 100 μM andrographolide (DENV2 + 100 μM ANDRO) and after 24 h proteins were prepared and subjected to western blot analysis to detect the expression of LC3 and actin. The antibody used recognises both the unlipidated (LC3-1) and lipidated (LC3-II) forms of LC3.

4. Discussion

Andrographolide is a labdene diterpenoid that has been shown to have activity against a wide range of viruses including positive sense single stranded RNA viruses such as hepatitis C virus [14], dengue virus [10,11] and chikungunya virus [12], negative-sense single-stranded segmented RNA viruses such as influenza A virus [9], double stranded DNA viruses such as hepatitis B virus [13] and herpes simplex virus [15,16], as well as the single-stranded, positive-sense retrovirus human immunodeficiency virus [17,18]. The wide variety of viruses whose replication is affected by andrographolide suggests that the anti-viral activity of andrographolide is generated by effects upon the host cell, rather than through effects on the virus *per se*.

Andrographolide has been shown to exert effects upon a number of cellular pathways including autophagy [13,20], mitochondrial function [21], the unfolded protein response (UPR) pathway [22,23], and oxidative stress [24] and affecting any of these processes could easily impact upon viral replication, and impacting upon several processes at the same time could have profound anti-viral effects. Andrographolide has been proposed to exert its activity through covalent linkage with target compounds [39], and a number of directly targeted proteins have been identified including actin [19] and the p50 subunit of NF-κB [19,40]. In our study expression of NF-κB was reduced in a dose dependent manner after treatment with andrographolide, albeit not significantly. NF-κB is activated during DENV infection where it promotes cytokine production [41] and cell death [42], but it is unclear whether inhibition of this protein would have direct antiviral effects.

Previous proteomic studies have focused on either finding direct protein targets of andrographolide [19,40], or on investigating the broad effects of andrographolide on protein expression [20,21] as undertaken here in the GeLC-MS/MS portion of the study, and both types of studies have noted significant cell type specific effects [40,43].

In a study investigating the effects of andrographolide, Cheung and colleagues identified 65 proteins as differentially regulated in response to andrographolide treatment in both Hela and HepG2 cells [43]. The most significantly up-regulated protein was heme oxygenase 1, and studies have shown that heme oxygenase 1 has potent anti-dengue virus activity [11]. Similarly, Yi and colleagues have also proposed that andrographolide up-regulates heme oxygenase I [24], however, in our study, heme oxygenase 1 was not shown to be up-regulated by treatment of andrographolide, again suggesting that cell type specificity mediates the action of andrographolide.

The proteins identified in our study by treatment of andrographolide alone were predominantly associated with the response to stress, and a number of chaperone proteins were observed to be differentially regulated. In particular, while GRP78 was initially identified as differentially regulated by andrographolide treatment, it did not validate in the subsequent western blot analysis. However, GRP78 was also detected as differentially expressed in the 2D gel analysis, where it was significantly down-regulated in dengue-infected, andrographolide treated cells. Previous studies have shown that GRP78 is up-regulated in response to DENV infection [44–46], and while we saw no up-regulation in DENV infected cells in this study, our previous studies have shown that up-regulation is observable from day 2 post-infection [44], a later time point than examined in this study. Importantly, studies have shown that GRP78 facilitates DENV replication [46], and as such down-regulation of this protein will detrimentally affect DENV replication.

In addition to functioning as a chaperone that assists in protein folding in the ER, GRP78 is a critical mediator of the unfolded protein response [34], and DENV manipulates this machinery to benefit its viral production [47]. While it is possible that andrographolide interacts directly with GRP78, gene expression analysis showed significant alteration of gene expression of GRP78. While there was an early up-regulation of GRP78 expression, by 24 h.p.i. expression of GRP78 was significantly decreased in andrographolide treated infected cells as compared to andrographolide treated cells. While this broadly correlates with the protein profile, it suggests that andrographolide may impact upon a process that mediates GRP78 gene expression.

As noted above, GRP78 acts as a critical mediator of the unfolded protein response where it governs the activity of three UPR sensor molecules, namely IRE1, ATF6 and PERK. Under conditions of ER stress, GRP78 releases these three molecules, leading to their activation and induction of down-stream processes such as up-regulation of chaperone molecules, including GRP78 itself, up-regulation of ERAD genes and down-regulation of protein translation [34]. In particular, activation of PERK leads to phosphorylation of eIF2α which represses protein translation [48]. Interestingly, a significant increase in eiF2α phosphorylation was seen in response to andrographolide treatment of cells, and increased PERK phosphorylation was also demonstrated.

In addition to the effects on GRP78 and the unfolded protein response, dysregulation of proteins involved in glycolysis, the tricarboxylic acid cycle and oxidative phosphorylation were also

observed. Andrographolide was shown to reduce GAPDH protein expression significantly in andrographolide treated, infected cells which would tend to reduce glycolosis in the cell, with a concomitant effect on energy production which would impact upon DENV replication. Several studies have shown that autophagy is induced as a consequence of DENV infection [35,36]. We confirmed here an increase in the lipidated form of LC3, a marker of autophagy [49]. Similarly, studies have shown that andrographolide induces autophagy [20,37,38]. While the induction of autophagy by DENV has been shown to facilitate DENV replication [35,36] it is possible that the markedly higher levels of lipidated LC3 seen here are consistent with a much higher level of autophagy induction, which is possibly anti-DENV replication.

5. Conclusion

Combined, our results suggest that andrographolide impacts upon several processes that would tend to diminish DENV replication. In our previous work, we showed that andrographolide treatment resulted in a complete loss of DENV protein expression for both chikungunya virus and dengue virus [10,12]. This would suggest that the increased phosphorylation of eIF2α occurring in response to andrographolide is a major determinant of the anti-DENV activity of andrographolide, and that this occurs as a consequence of the effects (directly or otherwise) of andrographolide on the critical regulator of the unfolded protein response, GRP78.

Contribution of authors

AP and DRS designed the experimental protocols and prepared the manuscript. AP, AH and PW carried out all experimental work. AP and SR were responsible for all proteomic analysis.

Conflict of interests

The authors declare that there are no conflicts of interests.

Acknowledgements

This work was supported by Mahidol University, and the Thailand Research Fund and Mahidol University (BRG6080006; IRN60W0002; IRG5780009). PW was, and AH is, supported by scholarships from the Thailand Graduate Institute of Science and Technology (TGIST).

Appendix A. Supplementary data

Supplementary material related to this article can be found, in the online version, at doi:https://doi.org/10.1016/j.biopha.2018.10.054.

References

[1] A.M. King, M.J. Adams, E.J. Lefkowitz, E.B. Carstens, Virus Taxonomy: IXth Report of the International Committee on Taxonomy of Viruses vol 9, (2012) San Diego, CA..
[2] D.J. Gubler, Dengue and dengue hemorrhagic fever, Clin. Microbiol. Rev. 11 (1998) 480–496.
[3] D.R. Smith, A. Khakpoor, Involvement of the liver in dengue infections, Dengue Bull. 33 (2009) 75–86.
[4] S.J. Balsitis, J. Coloma, G. Castro, A. Alava, D. Flores, J.H. McKerrow, P.R. Beatty, E. Harris, Tropism of dengue virus in mice and humans defined by viral nonstructural protein 3-specific immunostaining, Am. J. Trop. Med. Hyg. 80 (2009) 416–424.
[5] K.S. Aye, K. Charngkaew, N. Win, K.Z. Wai, K. Moe, N. Punyadee, S. Thiemmeca, A. Suttitheptumrong, S. Sukpanichnant, M. Prida, S.B. Halstead, Pathologic highlights of dengue hemorrhagic fever in 13 autopsy cases from Myanmar, Hum. Pathol. 45 (2014) 1221–1233.
[6] C.H. Kuo, D.I. Tai, C.S. Chang-Chien, C.K. Lan, S.S. Chiou, Y.F. Liaw, Liver biochemical tests and dengue fever, Am. J. Trop. Med. Hyg. 47 (1992) 265–270.
[7] S. Akbar, Andrographis paniculata: a review of pharmacological activities and clinical effects, Altern. Med. Rev. 16 (2011) 66–77.
[8] M.S. Hossain, Z. Urbi, A. Sule, K.M. Hafizur Rahman, Andrographis paniculata (Burm. f.) Wall. Ex Nees: a review of ethnobotany, phytochemistry, and pharmacology, Sci. World J. 2014 (2014) 274905.
[9] Y. Ding, L. Chen, W. Wu, J. Yang, Z. Yang, S. Liu, Andrographolide inhibits influenza A virus-induced inflammation in a murine model through NF-kappaB and JAK-STAT signaling pathway, Microb. Infect. 19 (2017) 605–615.
[10] P. Panraksa, S. Ramphan, S. Khongwichit, D.R. Smith, Activity of andrographolide against dengue virus, Antiviral Res. 139 (2017) 69–78.
[11] C.K. Tseng, C.K. Lin, Y.H. Wu, Y.H. Chen, W.C. Chen, K.C. Young, J.C. Lee, Human heme oxygenase 1 is a potential host cell factor against dengue virus replication, Sci. Rep. 6 (2016) 32176.
[12] P. Wintachai, P. Kaur, R.C. Lee, S. Ramphan, A. Kuadkitkan, N. Wikan, S. Ubol, S. Roytrakul, J.J. Chu, D.R. Smith, Activity of andrographolide against chikungunya virus infection, Sci. Rep. 5 (2015) 14179.
[13] H. Chen, Y.B. Ma, X.Y. Huang, C.A. Geng, Y. Zhao, L.J. Wang, R.H. Guo, W.J. Liang, X.M. Zhang, J.J. Chen, Synthesis, structure-activity relationships and biological evaluation of dehydroandrographolide and andrographolide derivatives as novel anti-hepatitis B virus agents, Bioorg. Med. Chem. Lett. 24 (2014) 2353–2359.
[14] J.C. Lee, C.K. Tseng, K.C. Young, H.Y. Sun, S.W. Wang, W.C. Chen, C.K. Lin, Y.H. Wu, Andrographolide exerts anti-hepatitis C virus activity by up-regulating haeme oxygenase-1 via the p38 MAPK/Nrf2 pathway in human hepatoma cells, Br. J. Pharmacol. 171 (2014) 237–252.
[15] S. Seubsasana, C. Pientong, T. Ekalaksananan, S. Thongchai, C. Aromdee, A potential andrographolide analogue against the replication of herpes simplex virus type 1 in vero cells, Med. Chem. 7 (2011) 237–244.
[16] C. Wiart, K. Kumar, M.Y. Yusof, H. Hamimah, Z.M. Fauzi, M. Sulaiman, Antiviral properties of ent-labdene diterpenes of Andrographis paniculata nees, inhibitors of herpes simplex virus type 1, Phytother. Res. 19 (2005) 1069–1070.
[17] C. Calabrese, S.H. Berman, J.G. Babish, X. Ma, L. Shinto, M. Dorr, K. Wells, C.A. Wenner, L.J. Standish, A phase I trial of andrographolide in HIV positive patients and normal volunteers, Phytother. Res. 14 (2000) 333–338.
[18] V.L. Reddy, S.M. Reddy, V. Ravikanth, P. Krishnaiah, T.V. Goud, T.P. Rao, T.S. Ram, R.G. Gonnade, M. Bhadbhade, Y. Venkateswarlu, A new bis-andrographolide ether from Andrographis paniculata nees and evaluation of anti-HIV activity, Nat. Prod. Res. 19 (2005) 223–230.
[19] J. Wang, X.F. Tan, V.S. Nguyen, P. Yang, J. Zhou, M. Gao, Z. Li, T.K. Lim, Y. He, C.S. Ong, Y. Lay, J. Zhang, G. Zhu, S.L. Lai, D. Ghosh, Y.K. Mok, H.M. Shen, Q. Lin, A quantitative chemical proteomics approach to profile the specific cellular targets of andrographolide, a promising anticancer agent that suppresses tumor metastasis, Mol. Cell Proteomics 13 (2014) 876–886.
[20] H. Lu, X.Y. Zhang, Y.Q. Wang, X.L. Zheng, Z. Yin, W.M. Xing, Q. Zhang, Andrographolide sodium bisulfate-induced apoptosis and autophagy in human proximal tubular endothelial cells is a ROS-mediated pathway, Environ. Toxicol. Pharmacol. 37 (2014) 718–728.
[21] W.M. Xing, T.J. Yuan, J.D. Xu, L.L. Gu, P. Liang, H. Lu, Proteomic identification of mitochondrial targets involved in andrographolide sodium bisulfite-induced nephrotoxicity in a rat model, Environ. Toxicol. Pharmacol. 40 (2015) 592–599.
[22] A. Banerjee, H. Ahmed, P. Yang, S.J. Czinn, T.G. Blanchard, Endoplasmic reticulum stress and IRE-1 signaling cause apoptosis in colon cancer cells in response to andrographolide treatment, Oncotarget (2016).
[23] L.L. Gu, X.Y. Zhang, W.M. Xing, J.D. Xu, H. Lu, Andrographolide-induced apoptosis in human renal tubular epithelial cells: roles of endoplasmic reticulum stress and inflammatory response, Environ. Toxicol. Pharmacol. 45 (2016) 257–264.
[24] A.L. Yu, C.Y. Lu, T.S. Wang, C.W. Tsai, K.L. Liu, Y.P. Cheng, H.C. Chang, C.K. Lii, H.W. Chen, Induction of heme oxygenase 1 and inhibition of tumor necrosis factor alpha-induced intercellular adhesion molecule expression by andrographolide in EA.hy926 cells, J. Agric. Food Chem. 58 (2010) 7641–7648.
[25] P. Sithisarn, L. Suksanpaisan, C. Thepparit, D.R. Smith, Behavior of the dengue virus in solution, J. Med. Virol. 71 (2003) 532–539.
[26] E.A. Henchal, M.K. Gentry, J.M. McCown, W.E. Brandt, Dengue virus-specific and flavivirus group determinants identified with monoclonal antibodies by indirect immunofluorescence, Am. J. Trop. Med. Hyg. 31 (1982) 830–836.
[27] M.M. Bradford, A rapid and sensitive method for the quantitation of microgram quantities of protein utilizing the principle of protein-dye binding, Anal. Biochem. 72 (1976) 248–254.
[28] A. Shevchenko, H. Tomas, J. Havlis, J.V. Olsen, M. Mann, In-gel digestion for mass spectrometric characterization of proteins and proteomes, Nat. Protoc. 1 (2006) 2856–2860.
[29] A. Paemanee, N. Wikan, S. Roytrakul, D.R. Smith, Application of GelC-MS/MS to proteomic profiling of Chikungunya virus infection: preparation of peptides for analysis, Methods Mol. Biol. 1426 (2016) 179–193.
[30] H. Mi, X. Huang, A. Muruganujan, H. Tang, C. Mills, D. Kang, P.D. Thomas, PANTHER version 11: expanded annotation data from Gene Ontology and Reactome pathways, and data analysis tool enhancements, Nucleic Acids Res. 45 (2017) D183–D189.
[31] W. Huang da, B.T. Sherman, R.A. Lempicki, Systematic and integrative analysis of large gene lists using DAVID bioinformatics resources, Nat. Protoc. 4 (2009) 44–57.
[32] W. Huang da, B.T. Sherman, R.A. Lempicki, Bioinformatics enrichment tools: paths toward the comprehensive functional analysis of large gene lists, Nucleic Acids Res. 37 (2009) 1–13.
[33] D. Szklarczyk, J.H. Morris, H. Cook, M. Kuhn, S. Wyder, M. Simonovic, A. Santos, N.T. Doncheva, A. Roth, P. Bork, L.J. Jensen, C. von Mering, The STRING database in 2017: quality-controlled protein-protein association networks, made broadly accessible, Nucleic Acids Res. 45 (2017) D362–D368.
[34] D.T. Rutkowski, R.J. Kaufman, A trip to the ER: coping with stress, Trends Cell Biol. 14 (2004) 20–28.
[35] Y.R. Lee, H.Y. Lei, M.T. Liu, J.R. Wang, S.H. Chen, Y.F. Jiang-Shieh, Y.S. Lin,

T.M. Yeh, C.C. Liu, H.S. Liu, Autophagic machinery activated by dengue virus enhances virus replication, Virology 374 (2008) 240–248.
[36] M. Panyasrivanit, A. Khakpoor, N. Wikan, D.R. Smith, Co-localization of constituents of the dengue virus translation and replication machinery with amphisomes, J. Gen. Virol. 90 (2009) 448–456.
[37] W. Chen, L. Feng, H. Nie, X. Zheng, Andrographolide induces autophagic cell death in human liver cancer cells through cyclophilin D-mediated mitochondrial permeability transition pore, Carcinogenesis 33 (2012) 2190–2198.
[38] J. Zhou, S.E. Hu, S.H. Tan, R. Cao, Y. Chen, D. Xia, X. Zhu, X.F. Yang, C.N. Ong, H.M. Shen, Andrographolide sensitizes cisplatin-induced apoptosis via suppression of autophagosome-lysosome fusion in human cancer cells, Autophagy 8 (2012) 338–349.
[39] C. Aromdee, Andrographolide: progression in its modifications and applications - a patent review (2012 - 2014), Expert Opin. Ther. Pat. 24 (2014) 1129–1138.
[40] L. Li, H. Wijaya, S. Samanta, Y. Lam, S.Q. Yao, In situ imaging and proteome profiling indicate andrographolide is a highly promiscuous compound, Sci. Rep. 5 (2015) 11522.
[41] J. Lang, D. Vera, Y. Cheng, H. Tang, Modeling dengue virus-hepatic cell interactions using human pluripotent stem cell-derived hepatocyte-like cells, Stem Cell Rep. 7 (2016) 341–354.
[42] J.C. Lin, S.C. Lin, W.Y. Chen, Y.T. Yen, C.W. Lai, M.H. Tao, Y.L. Lin, S.C. Miaw, B.A. Wu-Hsieh, Dengue viral protease interaction with NF-kappaB inhibitor alpha/beta results in endothelial cell apoptosis and hemorrhage development, J. Immunol. 193 (2014) 1258–1267.
[43] M.T. Cheung, R. Ramalingam, K.K. Lau, W.L. Chiang, S.K. Chiu, Cell type-dependent effects of andrographolide on human cancer cell lines, Life Sci. 91 (2012) 751–760.
[44] K. Jitobaom, N. Tongluan, D.R. Smith, Involvement of voltage-dependent anion channel (VDAC) in dengue infection, Sci. Rep. 6 (2016) 12.
[45] C. Thepparit, A. Khakpoor, S. Khongwichit, N. Wikan, C. Fongsaran, P. Chingsuwanrote, P. Panraksa, D.R. Smith, Dengue 2 infection of HepG2 liver cells results in endoplasmic reticulum stress and induction of multiple pathways of cell death, BMC Res. Notes 6 (2013) 372.
[46] S. Wati, M.L. Soo, P. Zilm, P. Li, A.W. Paton, C.J. Burrell, M. Beard, J.M. Carr, Dengue virus infection induces upregulation of GRP78, which acts to chaperone viral antigen production, J. Virol. 83 (2009) 12871–12880.
[47] J. Peña, E. Harris, Dengue virus modulates the unfolded protein response in a time-dependent manner, J. Biol. Chem. 286 (2011) 14226–14236.
[48] R.C. Wek, D.R. Cavener, Translational control and the unfolded protein response, Antioxid. Redox Signal. 9 (2007) 2357–2371.
[49] D.J. Klionsky, et al., Guidelines for the use and interpretation of assays for monitoring autophagy, Autophagy 12 (2016) 1–222.